Application of particle swarm optimization for gravity inversion of 2.5-D sedimentary basins using variable density contrast

Kunal Kishore Singh and Upendra Kumar Singh*

Department of Applied Geophysics, Indian School of Mines, Dhanbad-826004, India

Correspondence: *upendra.ism@gmail.com

Abstract

Particle swarm optimization (PSO) is a global optimization technique that works similarly to swarms of birds searching for food. A Matlab code in PSO algorithm is developed to estimate the depth to the bottom of a 2.5-D sedimentary basin and coefficients of regional background from observed gravity anomalies. The density contrast within the source is assumed to be varying parabolically with depth. Initially, the PSO algorithm is applied on synthetic data with and without some Gaussian noise and its validity is tested by calculating the depth of the Gediz Graben, Western Anatolia and Godavari sub-basin, India. The Gediz Graben consists of Neogen sediments and the metamorphic complex forms the basement of the Graben. A thick uninterrupted sequence of Permian-Triassic and partly Jurassic and Cretaceous sediments forms the Godavari sub-basin. The PSO results are better correlated with results obtained by Marquardt method and borehole information.

Keywords: Particle swarm optimization, Sedimentary basin, Gravity anomaly, Inversion, Gaussian noise.

Introduction

Gravity method is a natural source method which helps in locating masses of greater or lesser density than the surrounding formations. It is used as a reconnaissance survey in hydrocarbon exploration. Sedimentary basins, which are characterized by negative gravity anomalies, are

the location of almost all of the world's hydrocarbon reserves. Interpretation of gravity data is a mathematical process of trying to optimize the parameters of the initial model in order to get a good match to the observed data. Interpretation of gravity data is always associated with the ambiguity problem. Ambiguity in gravity anomalies can be overcome by assigning a mathematical geometry to the anomaly causing body with a known density contrast (Rama Rao and Murthy, 1978). Bott (1960) used stacked prism model to describe the cross-section of a sedimentary basin, whereas Talwani (1959) used the polygonal model to describe source geometry. The parabolic density function is used to remove the complications associated with exponential (Cordell, 1973), cubic (Garcia-Abdeslem, 2005) and quadratic (Gallardo-Delgado et al., 2003) density functions. The Marquardt inversion through residual gravity anomalies delineates the structure of a sedimentary basin by estimating regional background (Chakravarthi and Sundararajan, 2007). Several authors have developed 2D/2.5D local optimization techniques over the 2D/2.5D sedimentary basin (Annecchione et al., 2001; Barbosa et. al, 1999; Bhattacharya and Navolio, 1975; Gadirov et. al, 2016; Litinsky, 1989; Morgan and Grant, 1963; Murthy et al., 1988; Murthy, and Rao, 1989; Won and Bavis, 1987) to interpret gravity anomalies with constant density function. In many publications over 3D gravity field computation with an approximation of geological bodies by 3D polygonal horizontal prism was applied (Eppelbaum and Khesin, 2004; Khesin et al. 1996). Rao (1990) used a quadratic density function, which is comparatively reliable to analyze gravity anomalies over basins having a limited thickness, whereas Chakravarthi and Rao (1993) have done in modeling and inversion of gravity anomalies with quadratic density function.

Particle swarm optimization (PSO) is a robust stochastic optimization technique based on the movement and intelligence of swarms, which was developed by James Kennedy and Russell Eberhart (1995). PSO applies the concept of social optimization in problem solving in various fields. In this paper, a Matlab code based on PSO is developed to interpret the gravity

anomalies of 2.5-D sedimentary basins, where the density varies parabolically with depth. PSO analyzed results are consistent and more accurate with other techniques and also well agreement significantly with borehole information.

Theory

In the Bott's approach, sedimentary basin is approximated by a series of vertical prisms. The gravity anomaly g_b at any point on the profile AA' as shown in Figure 1.

$$g_b = \sum_{j=2}^{N-1} g_j\left(x_1, 0\right) + Cx + D \tag{1}$$

The gravity effect of l^{th} prism is given as

$$g\left(x_1, 0\right) = \int_{z=z_1}^{z_2} \int_{y=-a}^{a} \int_{x=-c}^{c} \frac{G\Delta\rho\left(z\right) z dx dy dz}{\left[\left(x - x_1\right)^2 + y^2 + z^2\right]^{3/2}} \tag{2}$$

The parabolic density function at any depth w is given by

$$\Delta\rho\left(w\right) = \frac{\Delta\rho_0^3}{\left(\Delta\rho_0 - \alpha w\right)^2} \tag{3}$$

Finally, after integration of Chakravarthi and Sundararajan (2006), the equation (2) becomes

$$g\left(x_1, 0\right) = -2G\Delta\rho_0^3 \left\{ \left\langle \frac{\alpha x_1 L}{p_4}\left(\frac{1}{p_2} + \frac{1}{p_3}\right) ln\frac{p_5}{p_6} + \frac{L}{2P_2} ln\frac{\left(K + x_1\right)}{\left(K - x_1\right)} + \frac{x_1}{2p_3} ln\frac{\left(K + L\right)}{\left(K - L\right)} + \frac{\Delta\rho_0}{\alpha}\left[\frac{1}{p_2} tan^{-1}\left(\frac{KL}{zx_1}\right) + \frac{1}{p_3} tan^{-1}\left(\frac{x_1 K}{zL}\right)\right] - \frac{1}{\alpha p_5} tan^{-1}\left(\frac{Lx_1}{zL}\right) \right\rangle_{x_1 - c}^{x_1 + c} \right\}_{z_1}^{z_2} \tag{4}$$

Where,

$$K = \left(x_1^2 + L^2 + z^2\right), p_1 = x_1^2 + L^2, p_2 = L^2\alpha^2 + \Delta\rho_0^2,$$

$$p_3 = x_1^2 + \Delta\rho_0^2, p_4 = \sqrt{\left(p_1\alpha^2 + \Delta\rho_0^2\right)}, p_5 = \Delta\rho_0^2 - \alpha z \quad \text{and}$$

$$p_6 = -2\left(\alpha K p_4 + p_1\alpha^2 + \Delta\rho_0\alpha z\right).$$

Here, *N* is the number of observations, *G* is the universal gravitational constant, *C* and *D* are coefficients of regional background, *c* is half width of the prism, z_1 and z_2 are depths to the top and bottom of the basin, 2*L* is strike length of the prism, *a* is the offset of profile from the center of the prism and $\Delta\rho_0$ and α are constants of the parabolic density function at depth *z*.

Since profile AA' does not pass through the centers of each prism, equation 4 has to be calculated twice by putting *L-a* and *L+a* for *L* and taking the average. The initial depths of the basin calculated using observed anomaly g_0, is given by as

$$d_i = \frac{g_0(x_i)\Delta\rho_0}{41.89\Delta\rho_0^2 + \alpha g_0(x_i)}, i = 2,3,\ldots\ldots\ldots,N-1 \quad (5)$$

Profile AA' entirely covers the lateral dimensions of the sedimentary basin, therefore the depth of the basin on either side of the profile become zero. So, $d_1 = 0 = d_N$

Particle Swarm Optimization

PSO uses a number of particles (solutions) that constitute a swarm, moving around in the search space looking for the best solution. Each particle adjusts its "flying" according to its own flying experience as well as the flying experience of other particles. Each particle keeps track of its coordinates in the solution space which is associated with the best solution (fitness) that has achieved so far by that particle. This value is called personal best, Pbest. Another best value that is tracked by the PSO is the best value obtained so far by any particle in the neighborhood of that particle. This value is called global best, Gbest. The basic idea of PSO lies in accelerating each particle towards its Pbest and the Gbest locations with a random weighted acceleration at each time step (Mohapatra and Das, 2013).

$$V_t^k = w.V_t^{k-1} + c_1.rand_1.\left(Pbest_t - X_t^k\right) + c_2.rand_2.\left(Gbest - X_t^k\right) \quad (6)$$

$$X_t^k = X_t^{k-1} + V_t^k \quad (7)$$

where k is the number of iterations; t is the particle number; V_t^k is the velocity of the tth particle at k iterations; X_t^k is the position of t^{th} particle at k iterations; $Pbest_t$ is the best position of individual t^{th} particle (Local best position); $Gbest$ is the best position of all particles (Global best position); $rand_1$ and $rand_2$ are the independent uniformly random numbers in the range [0,1]; c_1 and c_2 are the positive learning factor which controls the maximum step length; w is the inertial weight factor that controls the speed of the particles. Equation (7) gives the updated velocity based on the current velocity, current position, local, best position and global best position. This process is repeated until the desired result is obtained. The schematic diagram/flow chart of PSO algorithm is shown in Figure 2.

Examples

The Matlab code based on PSO is applied to a synthetic model of a sedimentary basin and real field data sets from Gediz Graben, Western Anatolia and Godavari sub-basin, India.

Synthetic Example

We have used a synthetic gravity anomaly of 45×10^3m length at 1×10^3m station interval. In Bott's algorithm, the prism will be of equal width of 1×10^3m but with different strike lengths. Here parabolic density function is used with the constants $\Delta\rho_0 = -0.65\times10^3 \text{Kg}/\text{m}^3$ and $\alpha = 0.04\times10^3 \text{Kg}/\text{m}^3$ per 1000 m. The profile does not bisect the strike lengths of prism and so offset distance of the profile from the centre of each prism is mentioned in the code. We have added an interference term, $Ax+B$, with A = - 0.007 mgal per 1000 m and B = -10 mgal for the regional background. Required result is found at 15 iterations with RMS error of 2.9369e-006 from Marquardt algorithm.

We have used the same synthetic gravity anomaly for PSO algorithm. The Figure 3 shows the learning process of Pbest and G Best in terms of error and iterations. The best result is found with 57 iterations and 50 numbers of models (Figure 3). So it is seen that after 57 iterations and 50 models, the calculated anomalies match the synthetic anomaly and estimated depths coincide with the actual structure where RMS Error is 2.8383e-004. Gaussian noises of 5% and 10% are added to the synthetic data to perceive the robustness of the PSO algorithm. PSO does not find the true depths, but give values close to the true depths. The upper part of Figure 4 shows the synthetic and PSO calculated gravity anomalies of a synthetic model of a 2.5-D sedimentary basin and the lower part shows the inferred depth structure obtained from PSO and Marquardt algorithm for synthetic data. Figure 5 and Figure 6 shows the synthetic data with 5% and 10% Gaussian noises and calculated gravity anomalies obtained from PSO algorithm and inferred depth structure obtained by PSO and Marquardt algorithm.

Field Example

Gediz Graben, Western Anatolia

The first field case study of the interpretation of gravity anomalies has been taken from Gediz Graben, Western Anatolia. The PSO technique has been applied using 29 vertical prisms, each with equal width of $2\times10^{3}\,\mathrm{m}$ but with different strike length, whereas Chakravarthi and Sundararajan (2007) used same prism and interpreted gravity anomaly by Marquardt algorithm using a parabolic density function whose constants are $\Delta\rho_0 = \text{-}1.407\times10^{3}\,\mathrm{Kg/m^3}$ and $\alpha = 2.26935\times10^{3}\,\mathrm{Kg/m^3}$ per 1000 m.. .

We have used a similar number of prisms in PSO to improve the results. So with 65 iterations and 50 models, we achieve a good fit between observed and PSO analyzed gravity

anomalies with RMS error of 0.0083. The maximum thickness of the graben is inferred as 1.87×10^{3}m that matches well with 1.8×10^{3}m as estimated by Sari and Salk (2002) as compared to 1.64×10^{3}m obtained by Chakravarthi and Sundararajan (2007). The upper part of Figure 7 shows the observed and PSO calculated gravity anomalies over Gediz Graben, Western Anatolia and the lower part show the inferred depth structure obtained from PSO and Marquardt algorithm.

Godavari sub-basin

The Godavari sub-basin is one of the major basins of Pranhita-Godavari valleys (Rao, 1982), whose approximate strike length is 220×10^{3}m. The gravity profile is taken for study from the residual bouguer gravity anomaly map of the Godavari sub-basin as shown in Figure 8. We have used 29 vertical prisms, each with equal widths of 2×10^{3}m but with different strike length for sedimentary basin modeling. The constants of parabolic density functions used for Godavari sub-basin are $\Delta\rho_0 = -0.5\times10^{3}\,\mathrm{Kg/m^3}$ and $\alpha = 0.1518259\times10^{3}\,\mathrm{Kg/m^3}$ per 1000 m (Chakravarthi and Sundararajan, 2004). So with 71 iterations and 45 models, we achieve a good fit between observed and PSO analyzed gravity anomalies. The RMS error is 0.0099. The maximum depth of the basin, obtained from PSO is 4.09×10^{3}m which is quite close to the borehole information (Agarwal, 1995). Chakravarthi and Sundararajan (2005) obtained maximum depth of 4.0×10^{3}m whereas Ramanamurty and Parthasarathy (1988) suggested 4.5×10^{3}m as the thickness of the basin. The upper part of Figure 9 shows the variation of observed and PSO calculated gravity anomalies of Godavari sub-basin and the lower part shows the inferred structure obtained from PSO and Marquardt algorithm.

Conclusions

Particle swarm optimization (PSO) on Matlab environment is developed to estimate the model parameters of a 2.5-D sedimentary basin where the density contrast varies parabolically with depth. We have implemented the PSO algorithm on synthetic data with and without Gaussian noise and two field data sets. An observation has made that PSO is affected by some levels of noise, but estimated depths are close to the true depths. The results obtained from PSO using synthetic and field gravity anomalies are well correlated with borehole samples and provide more geological viable. Despite its long computation time, PSO is very simple to implement and is controlled by only one operator.

Acknowledgements

The authors express their sincere thanks to Prof. Dr. Lev Eppelbaum (Associate Editor), Dr. V. G. Gadirov (Referee) and one more anonymous referee for their constructive criticism leading to significant improvement in our manuscript. First author Mr. Kunal K. Singh thanks to IIT(ISM), Dhanbad (Jharkhand), India for providing the financial support to develop the infrastructre.

References

Agarwal, B.P., 1995. Hydrocarbon prospects of the Pranhita-Godavari Graben, India. Proceedings of Petrotech 95,115-121.

Annecchione, M.A., Chouteau, M., Keating, P., 2001. Gravity interpretation of bedrock topography: the case of the Oak Ridges Moraine, Southern Ontario, Canada. Journal of Applied Geophysics 47, 63–81.

Barbosa, V.C.F., Silva, J.B.C., Medeiros, W.E., 1999. Stable inversion of gravity anomalies of sedimentary basins with non smooth basement reliefs and arbitrary density contrast variations. Geophysics 64, 754–764.

Bott, M.H.P., 1960. The use of rapid digital computing methods for direct gravity interpretation of sedimentary basins. Geophysical Journal of the Royal Astronomical Society 3, 63–67.

Bhattacharya, B. K., and Navolio, M. E., 1975. Digital convolution for computing gravity and magnetic anomalies due to arbitrary bodies, Geophysics, 40, 981-992.

Chakravarthi, V., and Rao, C. V., 1993. Parabolic density function in sedimentary basin modeling: 18th Annual Convention and Seminar on Exploration Geophysics, Expanded Abstracts, A16.

Chakravarthi, V., Sundararajan, N., 2004. Ridge regression algorithm for gravity inversion of fault structures with variable density. Geophysics 69 (6), 1394–1404.

Chakravarthi, V., Sundararajan, N., 2005. Gravity modeling of 2.5D sedimentary basins with density contrast varying with depth. Computer and Geosciences 31, 820-827.

Chakravarthi, V., Sundararajan, N., 2006. Gravity anomalies of 2.5D multiple prismatic structures with variable density: a Marquardt inversion. Pure and Applied Geophysics 163, 229–242.

Chakravarthi, V., Sundararajan, N., 2007. INV2P5DSB-A code for gravity inversion of 2.5-D sedimentary basins using depth dependent density. Computers and Geosciences 33, 449-456.

Cordell, L., 1973. Gravity analysis using an exponential density-depth function—San Jacinto Graben, California. Geophysics 38 (4), 684–690.

208 Eppelbaum, L.V. and Khesin, B.E., 2004. Advanced 3-D modelling of gravity field unmasks
209 reserves of a pyrite-polymetallic deposit: A case study from the Greater Caucasus.
210 First Break, 22, No. 11, 53-56.
211 Gadirov, V.G., Gadirov K.V., Gamidova, A.R., 2016. The deep structure of Yevlakh-
212 Agjabedi depression of Azerbaijan on the gravity-magnetometer investigations,
213 Geodynamics, 1(20), 133-143.
214 Gallardo-Delgado, L.A., Perez-Flores, M.A., Gomez-Trevino, E., 2003. A versatile algorithm
215 for joint inversion of gravity and magnetic data. Geophysics 68, 949–959.
216 Garcia-Abdeslem, J., 2005. The gravitational attraction of a right rectangular prism with
217 density varying with depth following a cubic polynomial. Geophysics 70, 39–42.
218 Kennedy, J., Eberhart, R., 1995. Particle Swarm Optimization: International Conference on
219 Neural Network, IEEE, IV, 1942-1948.
220 Khesin, B.E., Alexeyev, V.V. and Eppelbaum, L.V., 1996. Interpretation of Geophysical
221 Fields in Complicated Environments. Kluwer Academic Publishers (Springer), Ser.:
222 Modern Approaches in Geophysics, Boston - Dordrecht - London, 368 p.
223 Litinsky, V. A., 1989. Concept of effective density: key to gravity depth determinations for
224 sedimentary basins, Geophysics, 54**,** 1474-1482.
225 Marquardt, D.W., 1963. An algorithm for least squares estimation of nonlinear parameters.
226 Journal Society Indian Applied Mathematics 11, 431–441.
227 Mohapatra, P., Das, S., 2013. Stock market prediction using bio-inspired computing: A
228 survey. International journal of Engineering Science and Technology 5(4), 739-746.
229 Monteiro Santos, F.A., 2010. Inversion of self-potential of idealized bodies' anomalies using
230 particle swarm optimization. Computers & Geosciences 36, 1185-1190.

231 Morgan, N. A., and Grant, F. S., 1963. High-speed calculation of gravity and magnetic
232 profiles across two-dimensional bodies having an arbitrary cross-section, Geophysical
233 Prospecting, 11, 10 -15.
234 Murthy, I.V.R., Rao, S.J., 1989. A FORTRAN 77 program for inverting gravity anomalies of
235 two-dimensional basement structures. Computers and Geosciences 15, 1149–1156.
236 Murthy, I. V. R., Krishna, P. R., and Rao, S. J., 1988. A generalized computer program for
237 two-dimensional gravity modeling of bodies with a flat top or a flat bottom or
238 undulating over a mean depth, Journal of Association of Exploration Geophysicists, 9,
239 93-103.
240 Rama Rao, B.S.R., Murthy, I.V.R., 1978. Gravity and Magnetic Methods of Prospecting:
241 Arnold-Heinemann Publishers, New Delhi, India, 390pp.
242 Ramanamurty, B.V., Parthasarathy, E.V.R., 1988. On the evolution of the Godavari
243 Gondwana Graben, based on LANDSAT Imagery interpretation. Journal of the
244 Geological Society of India 32, 417–425.
245 Rao, C.S.R., 1982. Coal resources of Tamilnadu, Andhra Pradesh, Orissa and Maharashtra:
246 Bulletin of the Geological Survey of India 2, 1-103.
247 Rao, C.V., Pramanik, A.G., Kumar, G.V.R.K., Raju, M.L., 1994. Gravity interpretation of
248 sedimentary basins with hyperbolic density contrast. Geophysical Prospecting 42,
249 825–839.
250 Rao, D. B., 1990. Analysis of gravity anomalies of sedimentary basins by an asymmetrical
251 trapezoidal model with quadratic density function, Geophysics, 55, 226-231.
252 Sari, C., Salk, M., 2002. Analysis of gravity anomalies with hyperbolic density contrast: an
253 application to the gravity data of Western Anatolia. Journal of Balkan Geophysical
254 Society 5, 87–96.

Talwani, M., Worzel, J., Landisman, M., 1959. Rapid gravity computations for two dimensional bodies with application to the Mendocino submarine fracture zone. Journal of Geophysical Research 64 (1), 49–59.

Won, I. J., and Bevis, M., 1987. Computing the gravitational and magnetic anomalies due to a polygon: Algorithms and Fortran subroutines, Geophysics, 52, 232-238.

Figure Captions

Figure 1. The 2.5-D sedimentary basin and its approximation by juxtaposing prisms.

Figure 2. The detail schematic diagram/flow chart of PSO techniques.

Figure 3. Iteration verses RMS error of Pbest and Gbest using PSO technique through synthetic gravity anomaly.

Figure 4. Synthetic and Calculated gravity anomalies with parabolic density function due to a synthetic model of a 2.5-D sedimentary basin, obtained from PSO algorithm and inferred depth structure obtained from PSO and Marquardt algorithm.

Figure 5. Synthetic data with 5% Gaussian noise and calculated gravity anomalies obtained from PSO algorithm and inferred depth structure obtained from PSO and Marquardt algorithm.

Figure 6. Synthetic data with 10% Gaussian noise and calculated gravity anomalies obtained from PSO algorithm and inferred depth structure obtained for PSO algorithm and Marquardt algorithm.

Figure 7. Observed and calculated gravity anomalies with parabolic density function, Gediz Graben, Western Anatolia obtained from PSO algorithm and Inferred structure obtained from PSO and Marquardt algorithm.

Figure 8. Residual bouguer gravity anomaly map of Godavari sub-basin (modified after Chakravarthi and Sundararajan, 2005) and gravity anomaly profile taken for study.

Figure 9. Observed and calculated residual bouguer gravity anomalies of parabolic density function of Godavari sub-basin obtained from PSO algorithm and inferred depth structure from PSO and Marquardt algorithm.

Figure 1

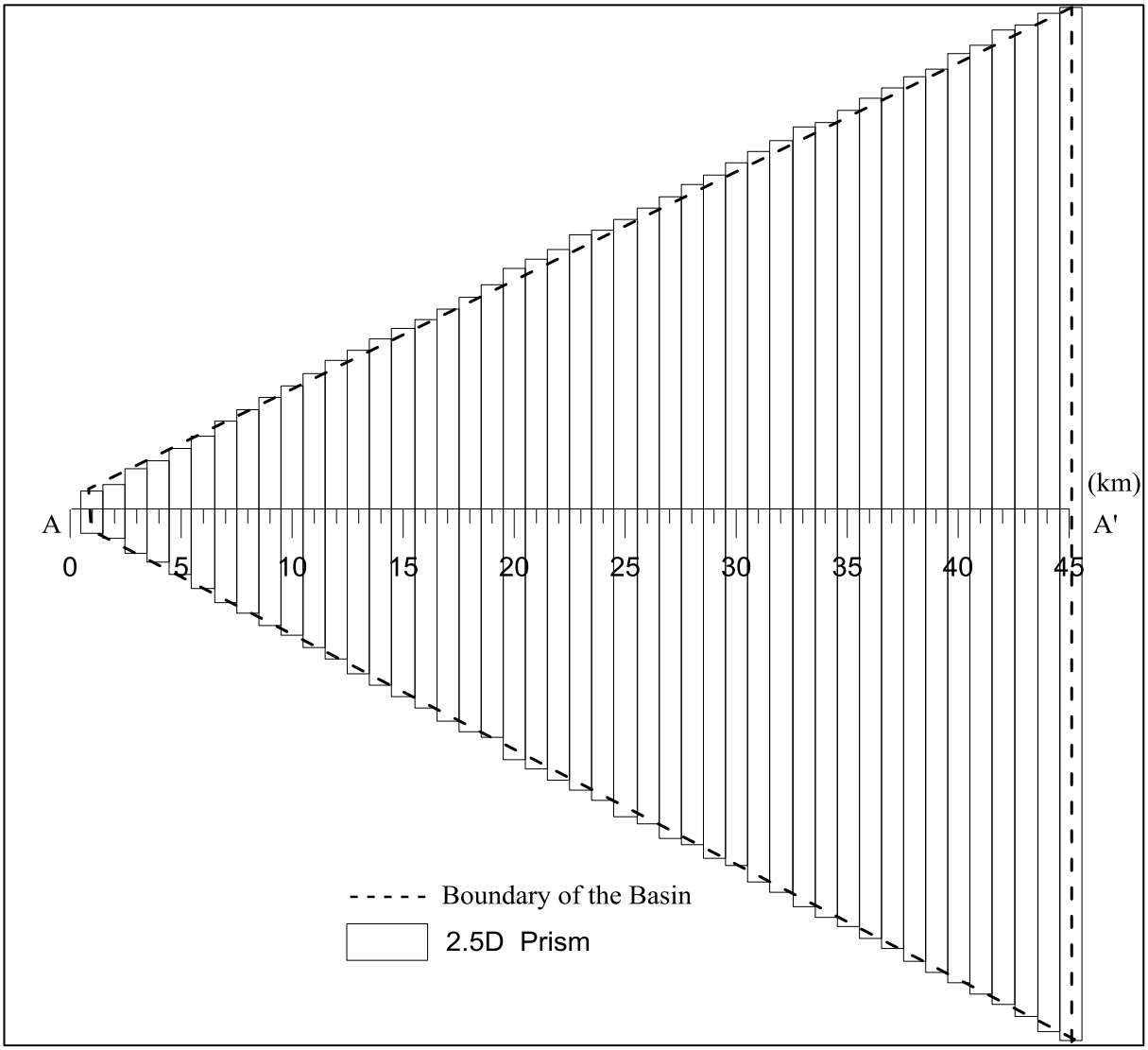

Figure 2

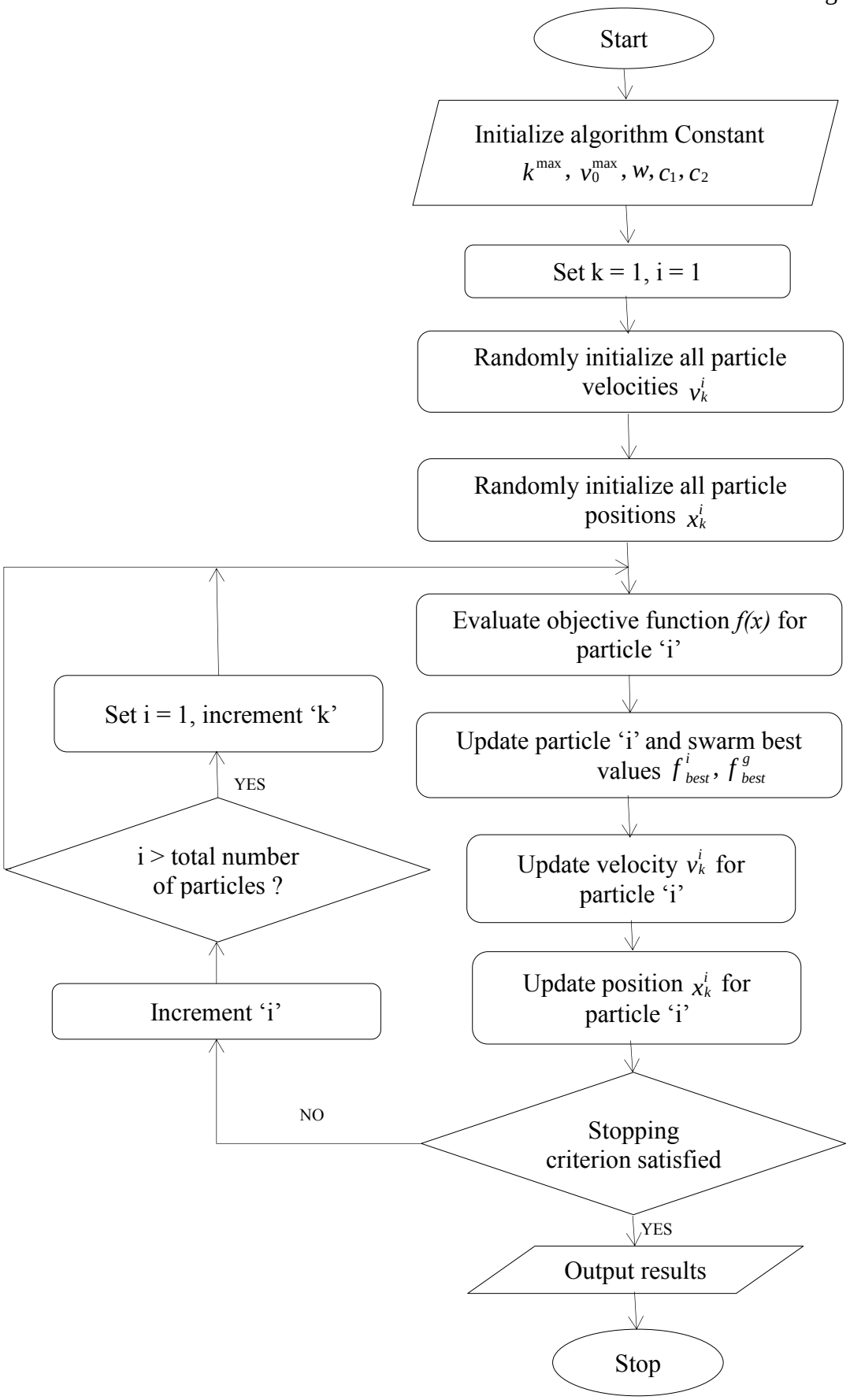
Start
Initialize algorithm Constant
k^{max}, v_0^{max}, w, c_1, c_2
Set k = 1, i = 1
Randomly initialize all particle velocities v_k^i
Randomly initialize all particle positions x_k^i
Evaluate objective function $f(x)$ for particle 'i'
Update particle 'i' and swarm best values f_{best}^i, f_{best}^g
Update velocity v_k^i for particle 'i'
Update position x_k^i for particle 'i'
Stopping criterion satisfied
NO
YES
Increment 'i'
i > total number of particles ?
YES
Set i = 1, increment 'k'
Output results
Stop

Figure 3


Iteration vs Error
Error
Iteration
Pbest
gbest
0
0.2
0.4
0.6
0.8
1
0
20
40
60
80
100
120
140
160
180
200

Figure 4

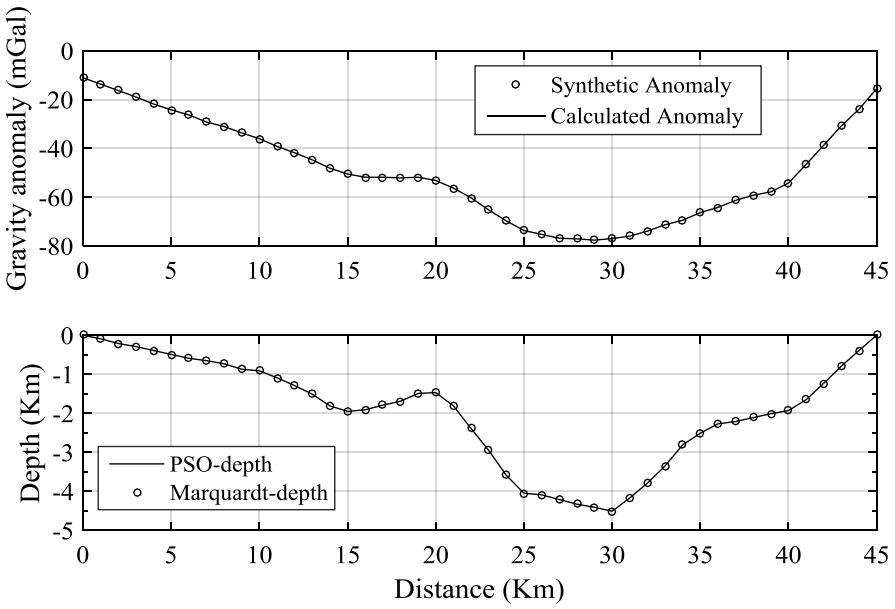
Gravity anomaly (mGal)
0
-20
-40
-60
-80
0
5
10
15
20
25
30
35
40
45
Synthetic Anomaly
Calculated Anomaly
Depth (Km)
0
-1
-2
-3
-4
-5
PSO-depth
Marquardt-depth
Distance (Km)

Figure 5

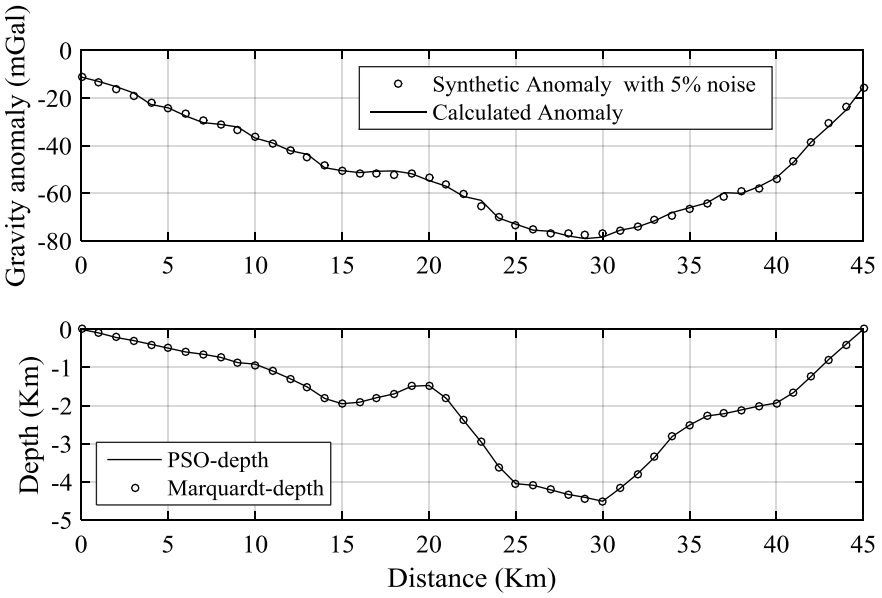
Gravity anomaly (mGal)
0
-20
-40
-60
-80
0
5
10
15
20
25
30
35
40
45
Synthetic Anomaly with 5% noise
Calculated Anomaly
Depth (Km)
0
-1
-2
-3
-4
-5
PSO-depth
Marquardt-depth
Distance (Km)

Figure 6

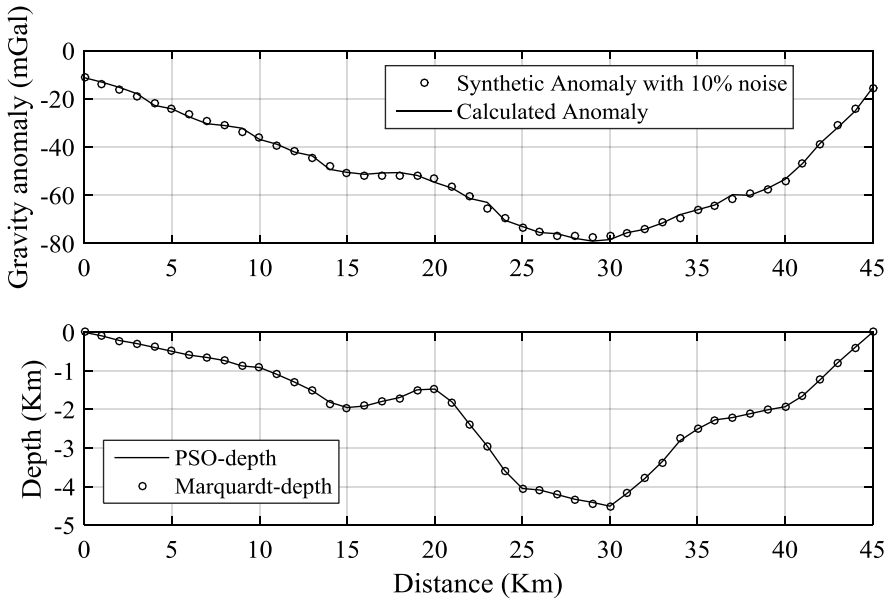
Gravity anomaly (mGal)
0
-20
-40
-60
-80
0
5
10
15
20
25
30
35
40
45
Synthetic Anomaly with 10% noise
Calculated Anomaly
Depth (Km)
0
-1
-2
-3
-4
-5
PSO-depth
Marquardt-depth
Distance (Km)

Figure 7

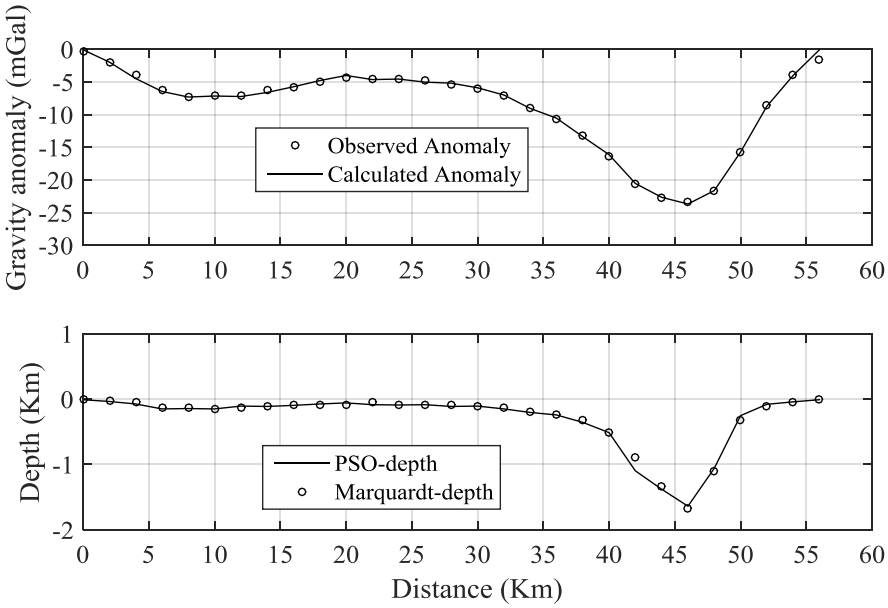
Gravity anomaly (mGal)
0
-5
-10
-15
-20
-25
-30
0 5 10 15 20 25 30 35 40 45 50 55 60
Observed Anomaly
Calculated Anomaly
Depth (Km)
1
0
-1
-2
0 5 10 15 20 25 30 35 40 45 50 55 60
PSO-depth
Marquardt-depth
Distance (Km)

Figure 8

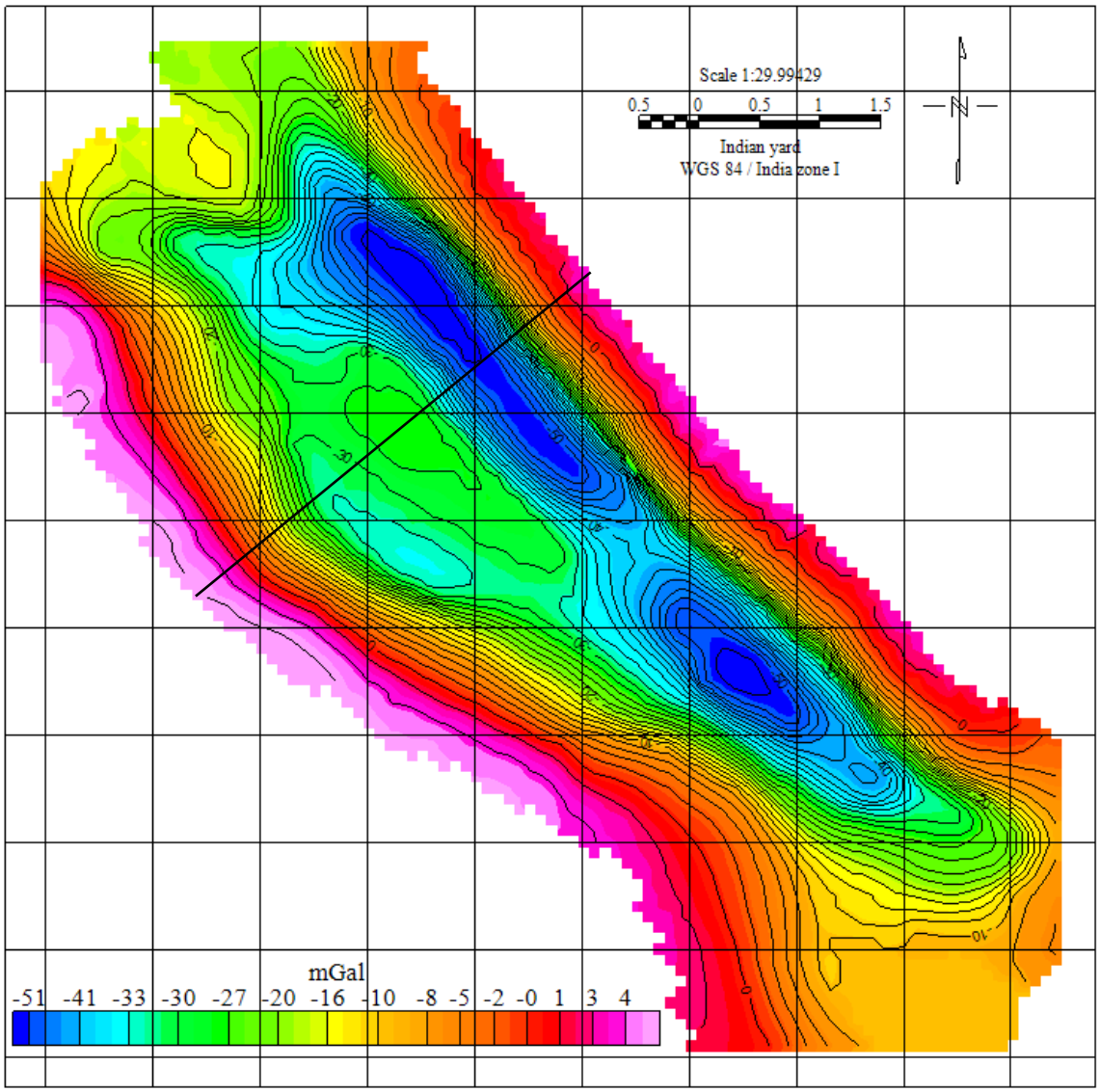
Scale 1:29.99429
0.5 0 0.5 1 1.5
Indian yard
WGS 84 / India zone I
N
mGal
-51 -41 -33 -30 -27 -20 -16 -10 -8 -5 -2 -0 1 3 4

Figure 9

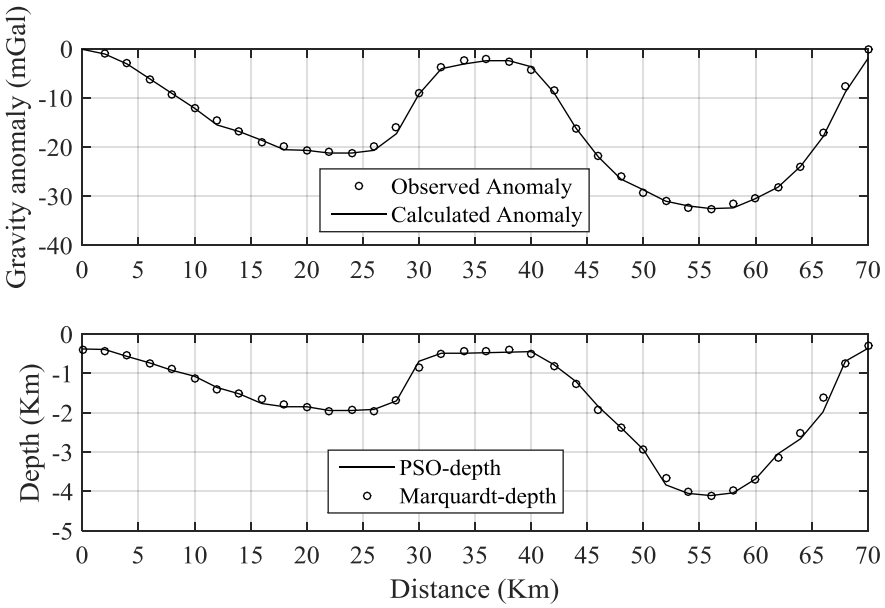
Gravity anomaly (mGal)
0
-10
-20
-30
-40
Observed Anomaly
Calculated Anomaly
0 5 10 15 20 25 30 35 40 45 50 55 60 65 70
Depth (Km)
0
-1
-2
-3
-4
-5
PSO-depth
Marquardt-depth
0 5 10 15 20 25 30 35 40 45 50 55 60 65 70
Distance (Km)